AMBIENT PRESSURE HYBRID SILICA MONOLITHS WITH HEXAMETHYLDISILAZANE: FROM VITREOUS HYDROPHILIC XEROGELS TO SUPERHYDROPHOBIC AEROGELS

Maria de Fátima Júlio[(1)] and Laura M. Ilharco[(1)*]

[(1)]Centro de Química-Física Molecular and Institute of Nanoscience and Nanotechnology, Instituto Superior Técnico, Universidade de Lisboa, Av. Rovisco Pais 1, 1049-001 Lisboa, Portugal

ELECTRONIC SUPPORTING INFORMATION

[*]To whom the correspondence should be addressed.

E-mail: lilharco@tecnico.ulisboa.pt

Deconvolution of the DRIFT spectra in the 700-1300 cm^{-1} region

The spectral deconvolutions were performed by a non-linear least squares fitting method, using the peak fitting module of OriginPro 7.0. Gaussian band profiles were assumed for all the components, except those related to methyl groups that were considered Lorentzian. No baseline corrections were made and no restrictions were imposed on the band positions and widths. The band positions were confirmed by the second derivative of the spectra. The best fits were obtained with $\chi^2 \approx 10^{-6}$ and correlation coefficient of 0.999.

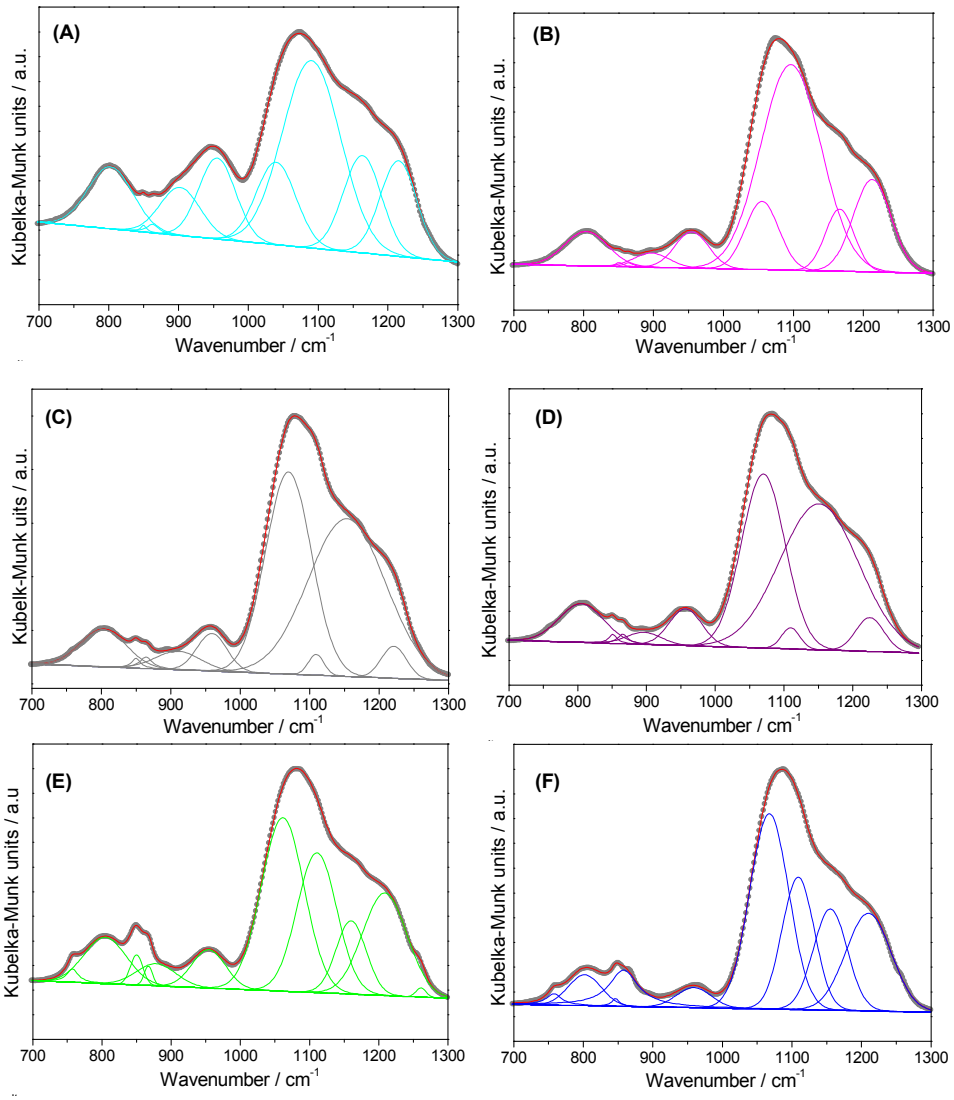

Figure S1. Deconvolution of the infrared spectra in the 700-1300 cm^{-1} region for samples $A_{0.011}$ (A), $A'_{0.011}$ (B), $A_{0.021}$ (C), $A'_{0.021}$ (D), $A_{0.054}$ (E) and $A'_{0.054}$ (F).

Table S1. Components obtained by deconvolution of the spectral region between 700 and 1300 cm^{-1} for the series A_a and A'_a.

	$\tilde{\nu}$ / cm^{-1} (Area /%)	$\tilde{\nu}$ / cm^{-1} (Area /%)	$\tilde{\nu}$ / cm^{-1} (Area /%)	$\tilde{\nu}$ / cm^{-1} (Area /%)	$\tilde{\nu}$ / cm^{-1} (Area /%)	$\tilde{\nu}$ / cm^{-1} (Area /%)	
Sample	**$A_{0.011}$**	**$A_{0.021}$**	**$A_{0.054}$**	**$A'_{0.011}$**	**$A'_{0.021}$**	**$A'_{0.054}$**	**Assignments**
Series A_a and A'_a	-	-	757 (0.87)	-	-	757 (1.06)	ρCH_3
	802 (9.54)	802 (6.37)	804 (7.99)	803 (6.34)	805 (7.21)	802 (4.38)	ν_sSi-O-Si
	849 (0.20)	849 (0.47)	849 (1.54)	850 (0.19)	850 (0.46)	846 (0.38)	γCH_3
	862 (0.49)	864 (0.78)	867 (0.67)	864 (0.23)	865 (0.59)	858 (6.38)	γCH_3
	902 (6.57)	910 (3.15)	878 (3.51)	897 (2.14)	896 (1.74)	959 (2.99)	νSi-O^-
	955 (10.17)	959 (4.24)	954 (5.22)	954 (5.22)	956 (4.99)	-	νSi-O(H)
	1039 (11.13)	1069 (35.01)	1061 (30.08)	1055 (9.83)	1069 (31.70)	1067 (32.77)	ν_{as}Si-O-Si [TO $(SiO)_6$]
	1090 (37.17)	1109 (1.24)	1110 (22.45)	1096 (53.34)	1109 (1.62)	1108 (18.35)	ν_{as}Si-O-Si [TO $(SiO)_4$]
	1163 (12.67)	1153 (45.68)	1160 (8.92)	1166 (7.68)	1151 (47.70)	1155 (14.74)	ν_{as}Si-O-Si [LO $(SiO)_4$]
	1215 (12.05)	1221 (3.03)	1208 (18.38)	1212 (15.01)	1224 (3.96)	1210 (18.94)	ν_{as}Si-O-Si [LO $(SiO)_6$]
	-	-	1261 (0.37)	-	-	-	δCH_3
A[νSi-OH]	16.75	7.39	8.73	7.36	6.74	2.99	
A[CH_3-related]	0.69	1.26	3.44	0.42	1.05	7.8	

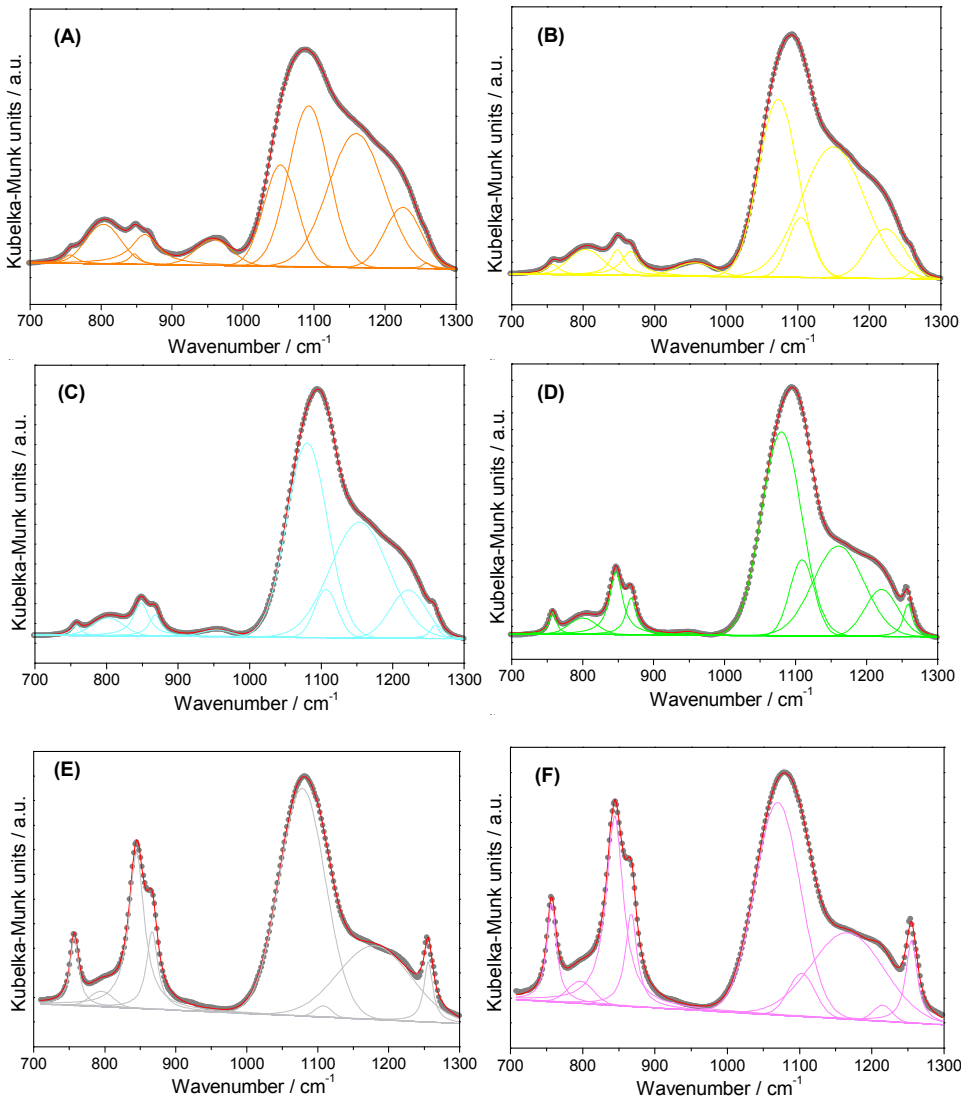

Figure S2. Deconvolution of the infrared spectra in the 700-1300 cm^{-1} region for samples $B_{0.021}$-t_{∞} (A), $B_{0.054}$-t_{∞} (B), $B_{0.107}$-t_{∞} (C), $B_{0.214}$-t_{∞} (D), $B_{0.428}$-t_{∞} (E) and $B_{0.857}$-t_{∞} (F).

Table S2. Components obtained by deconvolution of the spectral region between 700 and 1300 cm^{-1} for the series B_b-t_∞.

	$\tilde{\nu}$ / cm^{-1} (Area /%)	$\tilde{\nu}$ / cm^{-1} (Area /%)	$\tilde{\nu}$ / cm^{-1} (Area /%)	$\tilde{\nu}$ / cm^{-1} (Area /%)	$\tilde{\nu}$ / cm^{-1} (Area /%)	$\tilde{\nu}$ / cm^{-1} (Area /%)	
Sample	**$B_{0.021}$-t_∞**	**$B_{0.054}$-t_∞**	**$B_{0.107}$-t_∞**	**$B_{0.214}$-t_∞**	**$B_{0.428}$-t_∞**	**$B_{0.857}$-t_∞**	**Assignments**
Series B_b-t_∞	756 (0.65)-	757 (0.87)	757 (0.69)	757 (1.85)	757 (3.95)	756 (4.86)	ρCH_3
	803 (5.88)	803 (4.03)	802 (2.85)	800 (2.36)	795 (3.18)	796 (2.07)	ν_sSi-O-Si
	846 (0.68)	847 (2.51)	848 (3.76)	846 (6.29)	844 (13.03)	844 (17.15)	γCH_3
	861 (4.95)	866 (2.98)	868 (1.92)	868 (2.95)	866 (5.80)	867 (5.88)	γCH_3
	958 (3.96)	956 (2.36)	954 (1.04)	949 (0.21)	949 (0.33)	-	νSi-O(H)
	1052 (14.46)	1072 (32.45)	1080 (40.26)	1080 (42.79)	1076 (42.37)	1069 (42.19)	ν_{as}Si-O-Si [TO $(SiO)_6$]
	1092 (27.64)	1104 (7.22)	1106 (5.58)	1109 (9.86)	1107 (1.83)	1103 (1.75)	ν_{as}Si-O-Si [TO $(SiO)_4$]
	1159 (32.02)	1149 (38.68)	1153 (34.19)	1160 (24.07)	1167 (22.89)	1166 (21.18)	ν_{as}Si-O-Si [LO $(SiO)_4$]
	1225 (9.46)	1222 (8.52)	1222 (8.85)	1221 (8.09)	1218 (1.82)	1215 (1.11)	ν_{as}Si-O-Si [LO $(SiO)_6$]
	1258 (0.29)	1259 (0.38)	1258 (0.86)	1258 (2.19)	1255 (4.78)	1255 (3.82)	δCH_3
A[νSi-OH]	3.96	2.36	1.04	0.21	0.33	-	
A[CH_3-related]	6.27	6.35	6.37	11.09	22.78	27.9	

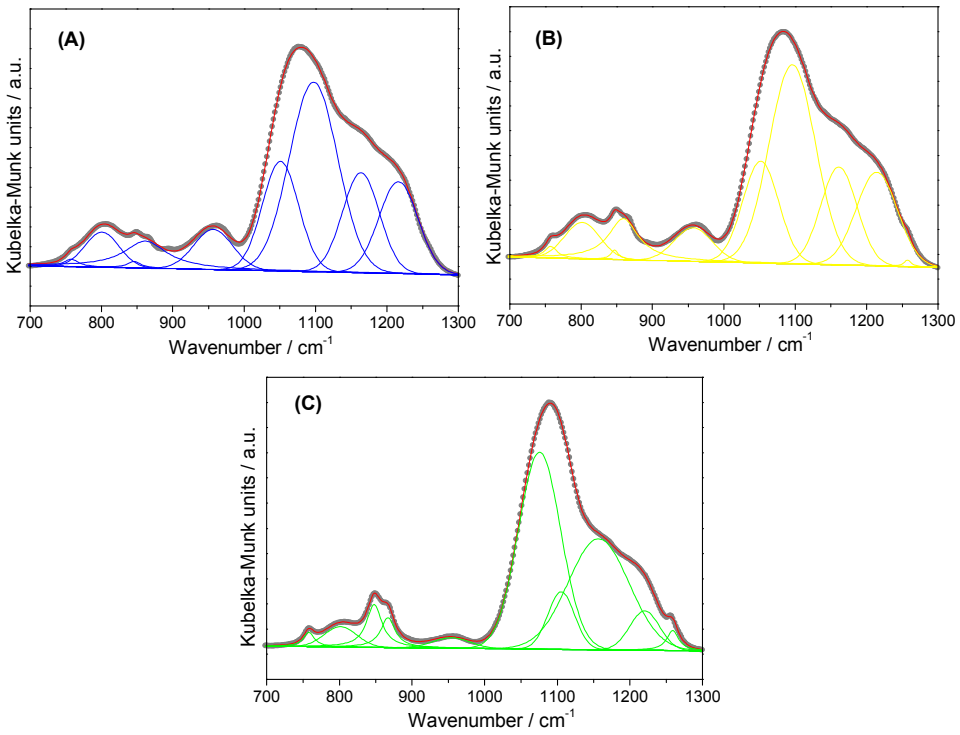

Figure S3. Deconvolution of the infrared spectra in the 700-1300 cm^{-1} region for samples $A_{0.0055}$-$B_{0.0055}$-t_∞ (A), $A_{0.0105}$-$B_{0.0105}$-t_∞ (B) and $A_{0.027}$-$B_{0.027}$-t_∞ (C).

Table S3. Components obtained by deconvolution of the spectral region between 700 and 1300 cm^{-1} for the series A_a-B_b-t_∞.

	$\tilde{\nu}$ / cm^{-1} (Area /%)	$\tilde{\nu}$ / cm^{-1} (Area /%)	$\tilde{\nu}$ / cm^{-1} (Area /%)	
Sample	**$A_{0.0055}$-$B_{0.0055}$-t_∞**	**$A_{0.0105}$-$B_{0.0105}$-t_∞**	**$A_{0.027}$-$B_{0.027}$-t_∞**	**Assignments**
Series A_a-B_b-t_∞	757 (0.59)-	757 (0.82)	757 (1.08)	ρCH_3
	801 (4.79)	801 (5.13)	801 (3.15)	ν_sSi-O-Si
	846 (0.51)	847 (0.44)	847 (4.59)	γCH_3
	861 (6.36)	859 (6.93)	866 (3.00)	γCH_3
	956 (6.21)	957 (5.11)	954 (1.86)	νSi-O(H)
	1051 (15.84)	1051 (14.68)	1075 (39.65)	ν_{as}Si-O-Si [TO $(SiO)_6$]
	1097 (36.61)	1095 (36.92)	1106 (7.33)	ν_{as}Si-O-Si [TO $(SiO)_4$]
	1163 (14.75)	1161 (14.22)	1156 (32.11)	ν_{as}Si-O-Si [LO $(SiO)_4$]
	1216 (14.34)	1214 (15.47)	1220 (5.62)	ν_{as}Si-O-Si [LO $(SiO)_6$]
	-	1257 (0.27)	1259 (1.59)	δCH_3
A[νSi-OH]	6.21	5.11	1.85	
A[CH_3-related]	7.46	8.20	8.68	

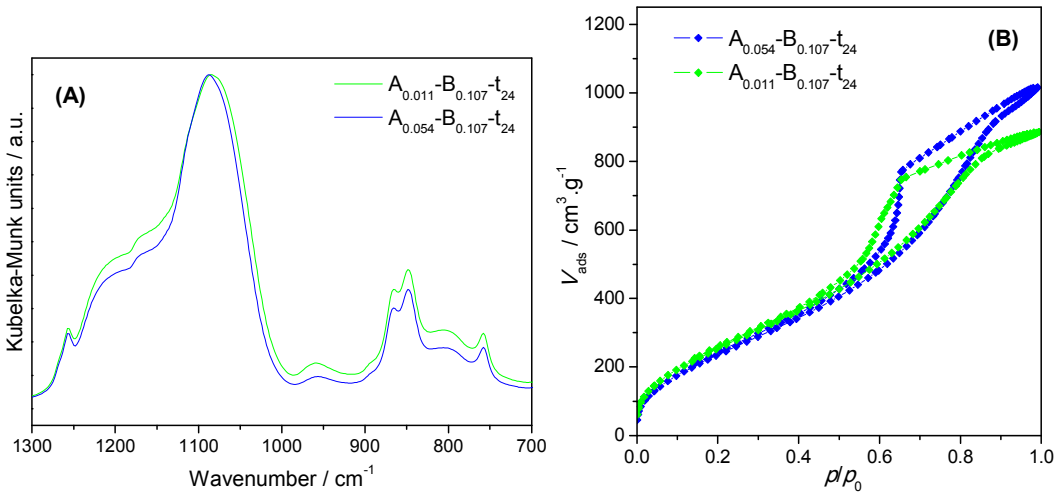

Figure S4. (A) DRIFT spectra of hybrid monoliths (series A_a-$B_{0.107}$-t_{24}) in the 700-1300 cm^{-1} region, normalized to the ν_{as}Si-O-Si band (at ~1090 cm^{-1}); (B) N_2 sorption isotherms of samples A_a-$B_{0.107}$-t_{24}.

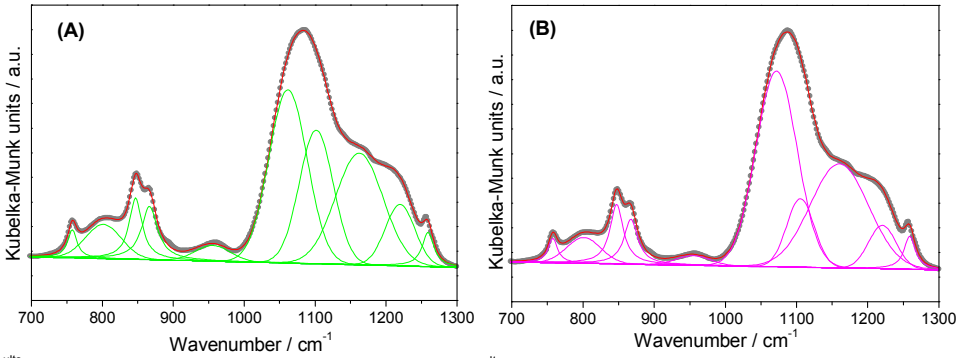

Figure S5. Deconvolution of the infrared spectra in the 700-1300 cm^{-1} region for samples $A_{0.011}$-$B_{0.107}$-t_{24} (A) and $A_{0.054}$-$B_{0.107}$-t_{24} (B).

Table S4. Components obtained by deconvolution of the spectral region between 700 and 1300 cm^{-1} for the series A_a-$B_{0.107}$-t_{24}.

Series A_a-$B_{0.107}$-t_{24}												
Sample	$\tilde{\nu}$ / cm^{-1} (Area /%)										**A[νSi-OH]**	**A[CH_3-related]**
$A_{0.011}$-$B_{0.107}$-t_{24}	757 (1.61)	801 (5.23)	846 (4.97)	866 (5.31)	955 (2.35)	1061 (28.44)	1101 (19.27)	1162 (22.64)	1219 (7.78)	1259 (2.39)	2.35	11.88
$A_{0.054}$-$B_{0.107}$-t_{24}	757 (1.54)	800 (4.13)	847 (5.44)	867 (4.24)	955 (1.53)	1071 (37.84)	1105 (8.84)	1160 (28.38)	1220 (5.64)	1259 (2.43)	1.53	11.21
Assignments	ρCH_3	ν_s Si-O-Si	γCH_3	γCH_3	ν Si-O(H)	ν_{as}Si-O-Si [TO $(SiO)_6$]	ν_{as}Si-O-Si [TO $(SiO)_6$]	ν_{as}Si-O-Si [TO $(SiO)_6$]	ν_{as}Si-O-Si [TO $(SiO)_6$]	δCH_3		